Experimental Observation of the Yang-Lee Quantum Criticality in Open Quantum Systems

Huixia Gao,[1,2] Kunkun Wang,[3] Lei Xiao,[2] Masaya Nakagawa,[4] Norifumi Matsumoto,[4] Dengke Qu,[1] Haiqing Lin,[5] Masahito Ueda,[4,6,7,*] and Peng Xue[2,1,†]

[1]*Beijing Computational Science Research Center, Beijing 100084, China*
[2]*School of Physics, Southeast University, Nanjing 211189, China*
[3]*School of Physics and Optoelectronic Engineering, Anhui University, Hefei 230601, China*
[4]*Department of Physics, University of Tokyo, 7-3-1 Hongo, Bunkyo-ku, Tokyo 113-0033, Japan*
[5]*School of Physics, Zhejiang University, Hangzhou 310030, China*
[6]*Institute for Physics of Intelligence, University of Tokyo, 7-3-1 Hongo, Bunkyo-ku, Tokyo 113-0033, Japan*
[7]*RIKEN Center for Emergent Matter Science (CEMS), Wako 351-0198, Japan*

(Received 6 September 2023; revised 25 February 2024; accepted 26 March 2024; published 24 April 2024)

The Yang-Lee edge singularity was originally studied from the standpoint of mathematical foundations of phase transitions. However, direct observation of anomalous scaling with the negative scaling dimension has remained elusive due to an imaginary magnetic field required for the nonunitary criticality. We experimentally implement an imaginary magnetic field with an open quantum system of heralded single photons, directly measure the partition function, and demonstrate the Yang-Lee edge singularity via the quantum-classical correspondence. We also demonstrate unconventional scaling laws for finite-temperature quantum dynamics.

DOI: 10.1103/PhysRevLett.132.176601

Introduction.—Yang-Lee zeros [1,2] are the zero points of the partition function that appear when some physical parameters are made complex and determine fundamental properties of phase transitions, such as critical exponents [3]. Yang and Lee [1,2] showed that zeros of the partition function of the classical ferromagnetic Ising model are distributed on the imaginary axis of the complex magnetic field [4–6] and related to singularities [7–16] in thermodynamic quantities. When the distribution of Yang-Lee zeros pinches (crosses) the real axis, the system exhibits a second-order (first-order) phase transition. Furthermore, the distribution itself exhibits singularity at its edges known as the Yang-Lee edge singularity [3,7–12], which is a prototypical example of nonunitary critical phenomena involving anomalous scaling laws unseen in unitary critical systems [17–20].

Yang-Lee zeros and Yang-Lee edge singularity have been extensively studied theoretically [21–26] and experimentally [27–35]. However, the imaginary magnetic field makes direct observation of the Yang-Lee edge singularity difficult and the physical meaning of the anomalous scaling accompanied by the negative scaling dimension elusive. Here the negative scaling dimension indicates that correlation functions diverge algebraically under space-time dilations and it is characteristic of nonunitary critical phenomena. A recent theoretical study [36] demonstrates that the Yang-Lee edge singularity can be implemented in quantum systems on the basis of the quantum-classical correspondence [37,38].

In this Letter, we experimentally implement an imaginary magnetic field and demonstrate the Yang-Lee edge singularity through a nonunitary evolution governed by a non-Hermitian Hamiltonian in an open quantum system. A quantum system exhibits the Yang-Lee zeros and the Yang-Lee edge singularity of the classical ferromagnetic Ising model due to the quantum-classical correspondence, where the nonunitary quantum criticality is identified with the singularity at an exceptional point. We also show unconventional scaling laws for finite-temperature dynamics. Furthermore, we present the phase diagram of the Yang-Lee quantum critical system, where Yang-Lee zeros appear in the parity-time ($\mathcal{PT}$)-broken phase. Our work is the first to measure all the critical exponents of the magnetization, the magnetic susceptibility, a two-time correlation function, and the density of zeros about the Yang-Lee edge singularity (see S7 of the Supplemental Material [39]). In particular, we directly observe the partition function, which gives a crucial advantage in the study of Yang-Lee zeros and related topics.

Yang-Lee edge singularity in open quantum systems.—We consider the Yang-Lee edge singularity in the classical one-dimensional Ising model with a pure-imaginary magnetic field $H = -J\sum_j \sigma_j\sigma_{j+1} - ih\sum_j \sigma_j$ [9], where $J > 0$, $h \in \mathbb{R}$, and $\sigma_j = \pm 1$. This model can be mapped to a quantum system governed by a $\mathcal{PT}$-symmetric non-Hermitian Hamiltonian [45,46]

$$H_{\mathcal{PT}} = R\cos\phi\sigma_x + iR\sin\phi\sigma_z \tag{1}$$

 © 2024 American Physical Society

via the quantum-classical correspondence [36], where $R > 0$, $\phi \in (-\pi/2, \pi/2)$, and σ_x and σ_z are the Pauli matrices. The partition function of H is obtained via the path-integral representation of its quantum counterpart. Matsumoto *et al.* [36] pointed out that the latter quantum system exhibits a criticality equivalent to the Yang-Lee edge singularity in the former classical system. The Hamiltonian $H_{\mathcal{PT}}$ satisfies the $\mathcal{PT}$ symmetry with $[H, \mathcal{PT}] = 0$, where $\mathcal{P} = \sigma_x$, $\mathcal{T} = \mathcal{K}$, and $\mathcal{K}$ is complex conjugation. The Hamiltonian $H_{\mathcal{PT}}$ has eigenenergies $E_\pm = \pm R\sqrt{\cos 2\phi}$ and the quantum critical points $\phi = \pm\pi/4$ corresponding to exceptional points [47,48], which separate the $\mathcal{PT}$-unbroken and broken regimes.

The Yang-Lee edge singularity occurs at the edges of the distribution of zeros of the partition function

$$Z = \mathrm{Tr}[e^{-\beta H_{\mathcal{PT}}}] = \sum_{p=\pm} e^{-\beta E_p}, \tag{2}$$

where β is the inverse temperature. The Yang-Lee quantum critical phenomena appear in the expectation value of a certain observable O given by [36,49–52]

$$\langle O \rangle = \frac{\mathrm{Tr}[O e^{-\beta H_{\mathcal{PT}}}]}{Z} = \frac{1}{Z} \sum_{p=\pm} \frac{\langle E_p^L | O | E_p^R \rangle}{\langle E_p^L | E_p^R \rangle} e^{-\beta E_p}, \tag{3}$$

where $|E_p^R\rangle$ ($\langle E_p^L|$) is the right (left) eigenvector of $H_{\mathcal{PT}}$. We simulate the $\mathcal{PT}$-symmetric nonunitary quantum dynamics using a single-photon interferometric network, and experimentally investigate the Yang-Lee quantum criticality.

Experimental demonstration.—To simulate the dynamics of the two-level $\mathcal{PT}$-symmetric system governed by $H_{\mathcal{PT}}$, we employ as the basis states the horizontal and vertical polarization states of a heralded single photon, i.e., $\{|0\rangle = |H\rangle, |1\rangle = |V\rangle\}$. Instead of implementing the non-Hermitian Hamiltonian $H_{\mathcal{PT}}$, we simulate the nonunitary quantum dynamics by directly implementing a nonunitary time-evolution operator U such that $U = e^{-iH_{\mathrm{eff}}t}$ at any given time t (see Eq. (5)). Here the effective non-Hermitian Hamiltonian is given by

$$H_{\mathrm{eff}} = H_{\mathcal{PT}} + \frac{d}{t}\mathbb{1}, \tag{4}$$

where $d = i \ln(1/\sqrt{\max|\lambda|})$, λ is the eigenvalue of $e^{-iH_{\mathcal{PT}}t} e^{iH_{\mathcal{PT}}^\dagger t}$ [53,54], and $\mathbb{1}$ is the 2×2 identity matrix. The probability amplitudes with respect to H_{eff} and $H_{\mathcal{PT}}$ are related to each other by $\langle j|e^{-iH_{\mathrm{eff}}t}|j\rangle = \langle j|e^{-iH_{\mathcal{PT}}t}|j\rangle/\sqrt{\max|\lambda|}$, where $j = H, V$.

The nonunitary operator U is implemented via the following decomposition (see also Fig. 1):

$$U = R(\phi_2, \theta_2, \phi_2')L(\theta_H, \theta_V)R(\phi_1, \theta_1, \phi_1'), \tag{5}$$

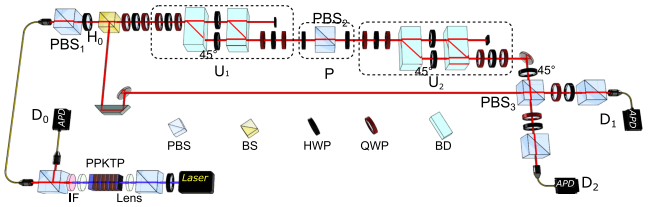

FIG. 1. Experimental setup. Heralded single photons are created via type-II spontaneous parametric down-conversion in a PPKTP crystal. The polarizing beam splitter PBS_1 and the half-wave plate (HWP) H_0 are used to generate initial polarization states $|H\rangle$ and $|V\rangle$. After photons pass through a 50:50 beam splitter (BS), the transmitted photons enter the evolution path, and the reflected photons act as reference photons and interfere with the transmitted photons at PBS_3. The evolution process involves nonunitary evolutions U_1 and U_2 realized by two beam displacers (BDs) and sets of wave plates and the projector P is realized by two HWPs and PBS_2. The measurement part involves PBS_3, two quarter-wave plates (QWPs), and two HWPs, followed by another two PBSs. Finally, photons are detected by avalanche photodiodes (APDs), and recorded by the coincidence counts of D_0, D_1, and D_0, D_2, respectively.

where the rotation $R(\phi_j, \theta_j, \phi_j')$ ($j = 1, 2$) can be realized by a set of sandwiched wave plates with a configuration quarter-wave plate (QWP) at ϕ_j, a half-wave plate (HWP) at θ_j, and a QWP at ϕ_j', and the polarization-dependent loss operator L is realized by a combination of two beam displacers (BDs) and two HWPs with setting angles θ_H and θ_V. For each given evolution time t, the nonunitary evolution U can be realized by tuning the setting angles of wave plates [55] and mapped to $e^{-iH_{\mathcal{PT}}t}$ with a correction factor $\sqrt{\max|\lambda|}$.

We characterize scaling laws of physical quantities for a finite-temperature quantum system via the magnetization

$$m = \langle \sigma_z \rangle = \frac{\langle H|e^{-\beta H_{\mathcal{PT}}}|H\rangle - \langle V|e^{-\beta H_{\mathcal{PT}}}|V\rangle}{\langle H|e^{-\beta H_{\mathcal{PT}}}|H\rangle + \langle V|e^{-\beta H_{\mathcal{PT}}}|V\rangle}, \tag{6}$$

the magnetic susceptibility

$$\chi = \frac{\mathrm{d}m}{\mathrm{d}a} = \frac{m - m'}{\tan\phi - \tan\phi'} \tag{7}$$

with $a = \tan\phi$ being a normalized magnetic field and m (m') representing the magnetization for $H_{\mathcal{PT}}(\phi)$ [$H_{\mathcal{PT}}(\phi')$], and the two-time correlation function

$$\begin{aligned} G(t_2, t_1) &= \langle \sigma_z(t_2)\sigma_z(t_1)\rangle - \langle \sigma_z(t_2)\rangle\langle \sigma_z(t_1)\rangle \\ &= \frac{1}{Z}\left(\Sigma_{HH}\Sigma'_{HH} - \Sigma_{HV}\Sigma'_{VH} - \Sigma_{VH}\Sigma'_{HV} + \Sigma_{VV}\Sigma'_{VV}\right) \\ &\quad - m^2, \end{aligned} \tag{8}$$

where $\Sigma_{ij} = \langle i|e^{-i\Delta t H_{\mathcal{PT}}}|j\rangle$, $\Sigma'_{ij} = \langle i|e^{(i\Delta t - \beta)H_{\mathcal{PT}}}|j\rangle$ ($i, j = H, V$), $\Delta t = t_2 - t_1$, and $Z = \langle H|e^{-\beta H_{\mathcal{PT}}}|H\rangle + \langle V|e^{-\beta H_{\mathcal{PT}}}|V\rangle$

is the partition function. We note that the finite-temperature scaling of $G(t_2, t_1)$ is unique to quantum critical phenomena.

As illustrated in Fig. 1, after single photons pass through a beam splitter (BS), transmitted photons as signal photons go through a nonunitary evolution, while the reflected photons as reference photons freely evolve and then interfere with the transmitted ones at the polarizing beam splitter PBS_3. Projective measurements with the bases of $\{|+\rangle, |-\rangle, |R\rangle\}$ $[|\pm\rangle = (|H\rangle \pm |V\rangle)/\sqrt{2},\ |R\rangle = (|H\rangle - i|V\rangle)/\sqrt{2}]$ are then performed on photons transmitted and reflected by the PBS. The outputs are recorded in coincidence with trigger photons. Typical measurements yield a maximum of 240 000 photon counts per second. For example, to measure m, we need to find both $\langle H|e^{-\beta H_{\mathcal{PT}}}|H\rangle$ and $\langle V|e^{-\beta H_{\mathcal{PT}}}|V\rangle$. Photons are initially prepared in the initial state $|H\rangle$ (or $|V\rangle$). After signal photons undergo a nonunitary evolution via $U = e^{-iH_{\text{eff}}t} = e^{-\beta H_{\mathcal{PT}}}/\sqrt{\max|\lambda|}$ (here we take $t = -i\beta$), they interfere with the reference photons in $|H\rangle$ (or $|V\rangle$) at PBS_3. The inverse temperature β is taken as a parameter of the nonunitary evolution and tuned by the setting angles of wave plates (see S3 of the Supplemental Material [39]). The overlap $\langle H(V)|e^{-\beta H_{\mathcal{PT}}}|H(V)\rangle$ can be calculated from coincidence counts (see S3 of the Supplemental Material [39]). Similarly, we can obtain the overlaps $\Sigma_{ij}\Sigma'_{ji}$ in $G(t_2, t_1)$ by applying nonunitary operations $U_1 = e^{-i\Delta t H_{\text{eff}}} = e^{-i\Delta t H_{\mathcal{PT}}}/\sqrt{\max|\lambda|}$ and $U_2 = e^{(i\Delta t-\beta)H_{\text{eff}}} = e^{(i\Delta t-\beta)H_{\mathcal{PT}}}/\sqrt{\max|\lambda|}$ and the projector $P = |j\rangle\langle j|$ on signal photons.

Yang-Lee critical phenomena.—We discuss the scaling laws of the system in the $\mathcal{PT}$-unbroken phase ($|\phi| < \pi/4$) by examining the dependence of physical quantities on $\Delta\phi := \pi/4 - \phi$. We consider two cases: (i) the limit $\phi \to \pi/4 - 0$ is taken after $1/\beta \to 0$; (ii) the limit $1/\beta \to 0$ is taken after $\phi \to \pi/4 - 0$. Here $\beta^{-1} = 0$ corresponds to the thermodynamic limit of the classical one-dimensional Ising model.

For case (i), the scaling laws are equivalent to those in the classical counterpart [9,36], i.e.,

$$m \to \frac{-i\sin\phi}{\sqrt{\cos 2\phi}} \propto \Delta\phi^{-\frac{1}{2}}, \qquad \chi \to \frac{-i\cos^3\phi}{\cos^{\frac{3}{2}}2\phi} \propto \Delta\phi^{-\frac{3}{2}},$$
$$G(t_2, t_1) \to \frac{\cos^2\phi}{\cos 2\phi}\exp\left[-2\pi i\frac{\Delta t}{\pi/(R\sqrt{\cos 2\phi})}\right]. \tag{9}$$

We experimentally test these scaling laws for $R = 0.05$, $\beta = 10^5$, and several values of $\Delta\phi$. Since the real parts of m and χ vanish, their scaling laws with respect to $\Delta\phi$ are characterized by their imaginary parts shown in Figs. 2(a) and 2(b). Fitting the power exponents to $m \sim \Delta\phi^{1/\delta}$ and $\chi \sim \delta\phi^{-\gamma}$, we obtain $1/\delta \sim -0.458 \pm 0.033$ and $\gamma \sim 1.477 \pm 0.350$, which agree with theoretical predictions $1/\delta = -1/2$ and $\gamma = 3/2$ in Eq. (9). Slight deviations from theoretical predictions are mainly due to the sensitivity

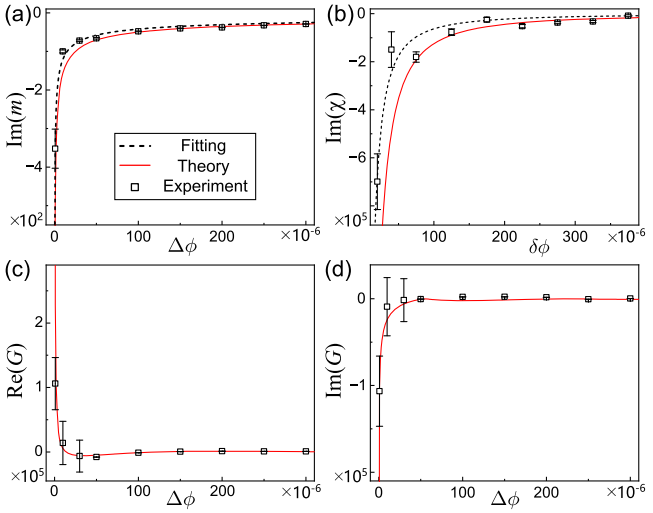

FIG. 2. Yang-Lee scaling laws of physical quantities for a finite-temperature quantum system in the $\mathcal{PT}$-unbroken phase in the limit $\phi \to \pi/4 - 0$ after $\beta^{-1} \to 0$. (a) Imaginary part of m as a function of $\Delta\phi$. (b) Imaginary part of χ as a function of $\delta\phi = (\Delta\phi + \Delta\phi')/2$, where $\Delta\phi = (10, 30, 50, 100, \ldots, 350) \times 10^{-6}$ and $\Delta\phi' = (30, 50, 100, 150, \ldots, 400) \times 10^{-6}$. Dependencies of real (c) and imaginary (d) parts of $G(t_2, t_1)$ on $\Delta\phi$. Experimental data are shown as open squares and theoretical predictions are represented by solid curves. We choose $R = 0.05$, $\beta = 10^5$, and $\Delta t = 3000$. Dashed curves in (a) and (b) correspond to the results fitted by different power laws. Error bars indicate the statistical deviation, obtained by Monte Carlo simulations under the assumption of Poissonian photon-counting statistics. Some error bars are smaller than the size of the symbols.

of the fitting result to the difference between the leftmost experimental data point in Fig. 2(a) and its theoretical prediction, where the slope of the curve becomes large. In Figs. 2(c) and 2(d), we also show the measured values of $G(t_2, t_1)$ with respect to $\Delta\phi$ for $\Delta t = 3000$, which agree with the theoretical predictions (see S4 of the Supplemental Material [39]).

For case (ii), we study the scaling laws

$$m \to -\frac{i}{\sqrt{2}}\beta R, \qquad \chi \to -\frac{i}{3\sqrt{2}}\left(\beta^3 R^3 + \frac{3}{2}\beta R\right),$$
$$G(t_2, t_1) \to R^2\left[\frac{1}{2}\beta^2 - i\beta\Delta t - (\Delta t)^2\right] + 1, \tag{10}$$

which have not been discussed in classical systems [9,36]. The critical exponents for the power-law dependence on β^{-1} are -1, -3, and -2. The two-time correlation function scales as $G(t_2, t_1) \propto (\Delta t)^2$ in the limit of $\Delta t \to \infty$. If Δt is replaced by an imaginary-time interval $-i\Delta\beta$, $G(t_2, t_1)$ becomes equivalent to the spatial correlation function $G_{\text{cl}}(x)$ of the classical system with the distance $x = \Delta\beta$. The power-law scaling $G_{\text{cl}}(x) \propto x^{-2\Delta} \propto x^{-(d_{\text{cl}}-2+\eta)}$ with a negative scaling dimension $\Delta = -1$ is consistent with

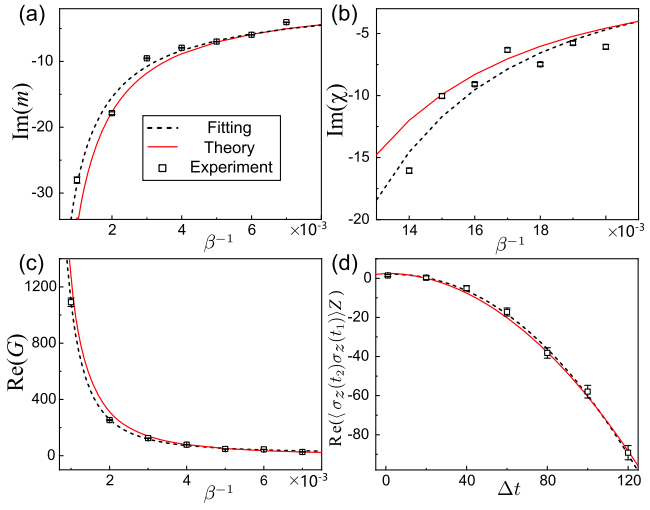

FIG. 3. Temperature dependences of anomalous scaling laws and Δt dependence of $\mathrm{Re}(\langle\sigma_z(t_2)\sigma_z(t_1)\rangle Z)$ in the limit of $\beta^{-1} \to 0$ after $\phi \to \pi/4 - 0$. Imaginary part of m (a) and that of χ (b) as functions of β^{-1}. (c) Real part of $G(t_2, t_1)$ as a function of β^{-1}. (d) Real part of $\langle\sigma_z(t_2)\sigma_z(t_1)\rangle Z$ as a function of Δt. We choose $R = 0.05$, $\phi = \pi/4$–10^{-6} ($\phi' = \pi/4$–10^{-2}), $\Delta t = 0.1$ in (a), (b), and (c), and $R = 0.05$, $\phi = \pi/4$–10^{-6}, $\beta = 10^4$ in (d).

the critical scaling in the corresponding one-dimensional ($d_{\mathrm{cl}} = 1$) classical system with anomalous dimension $\eta = -1$ [9]. To test this unconventional scaling laws, we choose $R = 0.05$, $\phi = \pi/4$–10^{-6} ($\phi' = \pi/4$–10^{-2}), and $\Delta t = 0.1$. By fitting the power exponents with $m \sim (\beta^{-1})^r$, $\chi \sim a(\beta^{-1})^{r'} + b(\beta^{-1})^r$, we obtain $r \sim -0.890 \pm 0.011$ and $r' \sim -3.171 \pm 0.062$, which agree with theoretical predictions -1 and -3 in Eq. (10). As illustrated in Fig. 3(c), by fitting the data with $G(t_2, t_1) \sim (\beta^{-1})^{r''}$, we obtain the experimental result $r'' \sim -2.160 \pm 0.021$, which is consistent with the theoretical prediction -2 in Eq. (10).

We also show the Δt dependence of $\langle\sigma_z(t_2)\sigma_z(t_1)\rangle Z$ with $\beta = 10^4$ in Fig. 3(d), which is equivalent to the dependence of $G(t_2, t_1)$ because Z and m are independent of Δt [see Eq. (8)]. The power exponent is fitted by $\langle\sigma_z(t_2)\sigma_z(t_1)\rangle Z \sim (\Delta t)^s$, and the obtained result is $s = 1 - \eta \sim 2.187 \pm 0.089$, which is consistent with the theoretical prediction $G(t_2, t_1) \sim (\Delta t)^2$.

Phase diagram and partition function.—In the $\mathcal{PT}$-broken phase ($|\phi| > \pi/4$), m, χ and $G(t_2, t_1)$ diverge periodically in the limit $\phi \to \pi/4 + 0$ after $\beta^{-1} \to 0$ [36]. The corresponding experimental data are shown in Sec. S4 of Supplemental Material [39]. The condition for divergence is

$$\beta R\sqrt{|\cos 2\phi|} = \left(n + \frac{1}{2}\right)\pi, \tag{11}$$

where n is an integer, which corresponds to the condition for zeros of the partition function

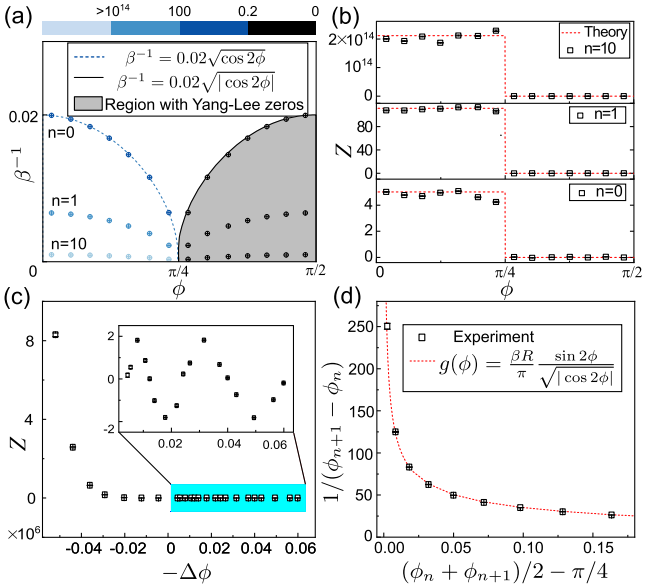

FIG. 4. (a) Phase diagram of the Yang-Lee quantum critical system. Experimental values of Z on the $\beta^{-1} - \phi$ plane. The critical point is located at $\phi = \pi/4$ and $\beta^{-1} = 0$. The Yang-Lee zeros appear in the $\mathcal{PT}$-broken ($\phi > \pi/4$) phase (gray region) given by Eq. (13). In the $\mathcal{PT}$-unbroken phase, a crossover between Yang-Lee scaling laws and unconventional scaling laws occurs around the region indicated by the blue-dashed curve. The experimental data are obtained with $n = 0$, $n = 1$, $n = 10$ from top to bottom, where n is given in Eq. (11), and the color indicates the value of Z. (b) Z as a function of ϕ for $n = 10$, $n = 1$, and $n = 0$. We choose $R = 0.01\pi$ for (a)–(b). For (c)–(d) we choose $R = 0.05$ and $\beta = 10^3$. (c) Z versus $-\Delta\phi$. The region colored in light blue shows the $\mathcal{PT}$-broken regime, and the inset is an enlarged view of the regime. (d) Density of zeros $1/(\phi_{n+1} - \phi_n)$ for $n = 0, 1, 2, \ldots, 9$ from left to right. The horizontal axis is taken as $(\phi_n + \phi_{n+1})/2$, which is measured from the critical point $\phi = \pi/4$.

$$Z = 2\cos\left(\beta R\sqrt{|\cos 2\phi|}\right), \tag{12}$$

i.e., the Yang-Lee zeros. These zeros appear only in the region defined by

$$\beta^{-1} \le \frac{2}{\pi} R\sqrt{|\cos 2\phi|}, \tag{13}$$

in the $\mathcal{PT}$-broken phase.

We measure the partition function Z on the $\beta^{-1} - \phi$ plane with $R = 0.01\pi$, $n = 0$, $n = 1$, and $n = 10$ in Eq. (11) for 14 different values of ϕ. As illustrated in Fig. 4(a), the Yang-Lee zeros appear only in the region of Eq. (13) in the $\mathcal{PT}$-broken phase. Figure 4(b) shows that Z takes large positive values in the $\mathcal{PT}$-unbroken phase and drops precipitously in the $\mathcal{PT}$-broken phase. Figure 4(c) shows that Z oscillates with $-\Delta\phi$ in the $\mathcal{PT}$-broken phase. Since the nodes of the oscillations correspond to Yang-Lee zeros, the oscillation period gives the distance between Yang-Lee zeros. Here, the observed value of the oscillation period

0.03 is consistent with the naive expectation value $\pi/100$, which is derived from Eq. (11) with the values of $\beta = 10^3$ and $R = 0.05$. Thus, we observe the Yang-Lee zeros experimentally and demonstrate that the Yang-Lee edge singularity manifests itself as the distribution of zeros of Z.

Density of zeros.—For the $(0+1)$-dimensional quantum Yang-Lee model in Eq. (1), the zero points $\{\phi_n\}_n$ of Z are determined from Eq. (11). The distribution of zeros becomes dense if the limit $\beta R \to \infty$ is taken. Calculating the density of zeros $g(\phi) \coloneqq \sum_n \delta(\phi - \phi_n)$, we find a power-law behavior

$$g(\phi) \propto (-\Delta\phi)^{\sigma} \tag{14}$$

with $\sigma = -1/2$ near the critical point $\phi = \pi/4$, consistent with the critical exponent $\sigma = 1/\delta = -1/2$ in the classical Yang-Lee edge singularity [3,9]. Figure 4(d) shows the experimental results of the density of zeros $1/(\phi_{n+1} - \phi_n)$ for $n = 0, 1, 2. \cdots, 9$ for $R = 0.05$ and $\beta = 10^3$, where the horizontal axis is measured from the critical point $\phi = \pi/4$. Our experimental results agree well with the analytic expression of $g(\phi) = (\beta R/\pi)(\sin 2\phi/\sqrt{|\cos 2\phi|})$ (see S1 of the Supplemental Material [39]). Via the density distribution of zeros experimentally observed for 10 different n's, we have achieved the direct observation of the Yang-Lee edge singularity.

Conclusion.—We have experimentally demonstrated the Yang-Lee singularity in a non-Hermitian quantum system with $\mathcal{PT}$ symmetry. Specifically, we have observed both anomalous scaling laws consistent with the classical Yang-Lee singularity and unconventional scaling laws that have not been discussed in classical systems. In particular, we directly observed the partition function in our experiment, which gives a decisive advantage in the study of Yang-Lee zeros and related topics. Our work presents the first experimental demonstration of the Yang-Lee quantum criticality in open quantum systems. We expect that the nonunitary critical phenomena in open quantum systems for higher-dimensional systems can also be probed (see S8 of the Supplemental Material [39]).

This work is supported by the National Key R&D Program of China (Grants No. 2023YFA1406701 and No. 2023YFA1406703) and the National Natural Science Foundation of China (Grants No. 92265209, No. 12025401, No. 12104009, No. 12104036, and No. 12305008). M. U. acknowledges support by KAKENHI Grant No. JP22H01152 from the Japan Society for the Promotion of Science and by the CREST program "Quantum Frontiers" (Grant No. JPMJCR23I1) by the Japan Science and Technology Agency. M. N. is supported by KAKENHI Grant No. JP20K14383 from the Japan Society for the Promotion of Science. N. M. is supported by KAKENHI Grant No. JP21J11280 from the Japan Society for the Promotion of Science. H. Q. L. acknowledges support from the National Natural Science Foundation of China (Grant No. 12088101). D. K. Q. acknowledges support from the China Postdoctoral Science Foundation (Grants No. BX20230036 and No. 2023M730198).

*ueda@cat.phys.s.u-tokyo.ac.jp
†gnep.eux@gmail.com

[1] C. N. Yang and T. D. Lee, Statistical theory of equations of state and phase transitions. I. Theory of condensation, Phys. Rev. **87**, 404 (1952).
[2] T. D. Lee and C. N. Yang, Statistical theory of equations of state and phase transitions. II. Lattice gas and Ising model, Phys. Rev. **87**, 410 (1952).
[3] M. E. Fisher, Yang-Lee edge singularity and ϕ^3 field theory, Phys. Rev. Lett. **40**, 1610 (1978).
[4] B. Simon and R. B. Griffiths, The $(\varphi^4)_2$ field theory as a classical Ising model, Commun. Math. Phys. **33**, 145 (1973).
[5] C. M. Newman, Zeros of the partition function for generalized Ising systems, Commun. Pure Appl. Math. **27**, 143 (1974).
[6] E. H. Lieb and A. D. Sokal, A general Lee-Yang theorem for one-component and multicomponent ferromagnets, Commun. Math. Phys. **80**, 153 (1981).
[7] P. J. Kortman and R. B. Griffiths, Density of zeros on the Lee-Yang circle for two Ising ferromagnets, Phys. Rev. Lett. **27**, 1439 (1971).
[8] D. A. Kurtze and M. E. Fisher, Yang-Lee edge singularities at high temperatures, Phys. Rev. B **20**, 2785 (1979).
[9] M. E. Fisher, Yang-Lee edge behavior in one-dimensional systems, Prog. Theor. Phys. Suppl. **69**, 14 (1980).
[10] J. L. Cardy, Conformal invariance and the Yang-Lee edge singularity in two dimensions, Phys. Rev. Lett. **54**, 1354 (1985).
[11] J. L. Cardy and G. Mussardo, S-matrix of the Yang-Lee edge singularity in two dimensions, Phys. Lett. B **225**, 275 (1989).
[12] A. B. Zamolodchikov, Two-point correlation function in scaling Lee-Yang model, Nucl. Phys. **B348**, 619 (1991).
[13] T. Sumaryada and A. Volya, Thermodynamics of pairing in mesoscopic systems, Phys. Rev. C **76**, 024319 (2007).
[14] T. Kist, J. L. Lado, and C. Flindt, Lee-Yang theory of criticality in interacting quantum many-body systems, Phys. Rev. Res. **3**, 033206 (2021).
[15] P. M. Vecsei, J. L. Lado, and C. Flindt, Lee-Yang theory of the two-dimensional quantum Ising model, Phys. Rev. B **106**, 054402 (2022).
[16] Kh. P. Gnatenko, A. Kargol, and V. M. Tkachuk, Two-time correlation functions and the Lee-Yang zeros for an interacting Bose gas, Phys. Rev. E **96**, 032116 (2017).
[17] R. Couvreur, J. L. Jacobsen, and H. Saleur, Entanglement in nonunitary quantum critical spin chains, Phys. Rev. Lett. **119**, 040601 (2017).
[18] P.-Y. Chang, J.-S. You, X. Wen, and S. Ryu, Entanglement spectrum and entropy in topological non-Hermitian systems and nonunitary conformal field theory, Phys. Rev. Res. **2**, 033069 (2020).

[19] C. Itzykson and J.-B. Zuber, Two-dimensional conformal invariant theories on a torus, Nucl. Phys. **B275**, 580 (1986).
[20] C. Itzykson, H. Saleur, and J.-B. Zuber, Conformal invariance of nonunitary 2d-models, Europhys. Lett. **2**, 91 (1986).
[21] A. Deger and C. Flindt, Determination of universal critical exponents using Lee-Yang theory, Phys. Rev. Res. **1**, 023004 (2019).
[22] A. Deger, F. Brange, and C. Flindt, Lee-Yang theory, high cumulants, and large-deviation statistics of the magnetization in the Ising model, Phys. Rev. B **102**, 174418 (2020).
[23] S. Peotta, F. Brange, A. Deger, T. Ojanen, and C. Flindt, Determination of dynamical quantum phase transitions in strongly correlated many-body systems using Loschmidt cumulants, Phys. Rev. X **11**, 041018 (2021).
[24] M. Heyl, Dynamical quantum phase transitions: A review, Rep. Prog. Phys. **81**, 054001 (2018).
[25] A. Connelly, G. Johnson, F. Rennecke, and V. V. Skokov, Universal location of the Yang-Lee edge singularity in O(N) theories, Phys. Rev. Lett. **125**, 191602 (2020).
[26] S. J. Jian, Z. C. Yang, Z. Bi, and X. Chen, Yang-Lee edge singularity triggered entanglement transition, Phys. Rev. B **104**, L161107 (2021).
[27] P. Jurcevic, H. Shen, P. Hauke, C. Maier, T. Brydges, C. Hempel, B. P. Lanyon, M. Heyl, R. Blatt, and C. F. Roos, Direct observation of dynamical quantum phase transitions in an interacting many-body system, Phys. Rev. Lett. **119**, 080501 (2017).
[28] N. Fläschner, D. Vogel, M. Tarnowski, B. S. Rem, D.-S. Lühmann, M. Heyl, J. C. Budich, L. Mathey, K. Sengstock, and C. Weitenberg, Observation of dynamical vortices after quenches in a system with topology, Nat. Phys. **14**, 265 (2018).
[29] C. Binek, W. Kleemann, and H. A. Katori, Yang-Lee edge singularities determined from experimental high-field magnetization data, J. Phys. Condens. Matter **13**, L811 (2001).
[30] B. B. Wei and R. B. Liu, Lee-Yang zeros and critical times in decoherence of a probe spin coupled to a bath, Phys. Rev. Lett. **109**, 185701 (2012).
[31] X. Peng, H. Zhou, B. B. Wei, J. Cui, J. Du, and R. B. Liu, Experimental observation of Lee-Yang zeros, Phys. Rev. Lett. **114**, 010601 (2015).
[32] K. Brandner, V. F. Maisi, J. P. Pekola, J. P. Garrahan, and C. Flindt, Experimental determination of dynamical Lee-Yang zeros, Phys. Rev. Lett. **118**, 180601 (2017).
[33] B. B. Wei, Probing Yang-Lee edge singularity by central spin decoherence, New J. Phys. **19**, 083009 (2017).
[34] B. B. Wei, Probing conformal invariant of non-unitary two dimensional systems by central spin decoherence, Sci. Rep. **8**, 3080 (2018).
[35] A. Francis, D. Zhu, C. Huerta Alderete, S. Johri, X. Xiao, J. K. Freericks, C. Monroe, N. M. Linke, and A. F. Kemper, Many-body thermodynamics on quantum computers via partition function zeros, Sci. Adv. **7**, eabf2447 (2021).
[36] N. Matsumoto, M. Nakagawa, and M. Ueda, Embedding the Yang-Lee quantum criticality in open quantum systems, Phys. Rev. Res. **4**, 033250 (2022).
[37] M. Suzuki, Relationship between d-dimensional quantal spin systems and $(d+1)$-dimensional Ising systems: Equivalence, critical exponents and systematic approximants of the partition function and spin correlations, Prog. Theor. Phys. **56**, 1454 (1976).
[38] J. B. Kogut, An introduction to lattice gauge theory and spin systems, Rev. Mod. Phys. **51**, 659 (1979).
[39] See the Supplemental Material at http://link.aps.org/supplemental/10.1103/PhysRevLett.132.176601 for more details about the theory background, the experimental implementation, additional experimental results, and the error analysis, which includes Refs. [40–44].
[40] L. Xiao, T. S. Deng, K. K. Wang, G. Y. Zhu, Z. Wang, W. Yi, and P. Xue, Non-Hermitian bulk-boundary correspondence in quantum dynamics, Nat. Phys. **16**, 761 (2020).
[41] K. K. Wang, L. Xiao, J. C. Budich, W. Yi, and P. Xue, Simulating exceptional non-Hermitian metals with single-photon interferometry, Phys. Rev. Lett. **127**, 026404 (2021).
[42] M. E. Fisher, The theory of equilibrium critical phenomena, Rep. Prog. Phys. **30**, 615 (1967).
[43] M. E. Fisher, Correlation functions and the critical region of simple fluids, J. Math. Phys. (N.Y.) **5**, 944 (1964).
[44] L. Xiao, D. K. Qu, K. K. Wang, H. W. Li, J. Y. Dai, B. Dóra, M. Heyl, R. Moessner, W. Yi, and P. Xue, Non-Hermitian Kibble-Zurek mechanism with tunable complexity in single-photon interferometry, PRX Quantum **2**, 020313 (2021).
[45] C. M. Bender and S. Boettcher, Real spectra in non-Hermitian Hamiltonians having PT symmetry, Phys. Rev. Lett. **80**, 5243 (1998).
[46] C. M. Bender, D. C. Brody, and H. F. Jones, Complex extension of quantum mechanics, Phys. Rev. Lett. **89**, 270401 (2002).
[47] M. V. Berry, Physics of non-Hermitian degeneracies, Czech. J. Phys. **54**, 1039 (2004).
[48] W. D. Heiss, The physics of exceptional points, J. Phys. A **45**, 444016 (2012).
[49] K. Uzelac, P. Pfeuty, and R. Jullien, Yang-Lee edge singularity from a real-space renormalization-group method, Phys. Rev. Lett. **43**, 805 (1979).
[50] G. Von Gehlen, Critical and off-critical conformal analysis of the Ising quantum chain in an imaginary field, J. Phys. A **24**, 5371 (1991).
[51] S. Yin, G.-Y. Huang, C.-Y. Lo, and P. Chen, Kibble-Zurek scaling in the Yang-Lee edge singularity, Phys. Rev. Lett. **118**, 065701 (2017).
[52] L. J. Zhai, G.-Y. Huang, and H.-Y. Wang, Pseudo-Yang-Lee edge singularity critical behavior in a non-Hermitian Ising model, Entropy **22**, 780 (2020).
[53] P. R. Halmos, Normal dilations and extensions of operators, Summ. Bras. Math. **2**, 125 (1950).
[54] C. Sparrow, E. Martin-Lopez, N. Maraviglia, A. Neville, C. Harrold, J. Carolan, Y. N. Joglekar, T. Hashimoto, N. Matsuda, J. L. O'Brien, D. P. Tew, and A. Laing, Simulating the vibrational quantum dynamics of molecules using photonics, Nature (London) **557**, 660 (2018).
[55] L. Xiao, K. K. Wang, X. Zhan, Z. H. Bian, K. Kawabata, M. Ueda, W. Yi, and P. Xue, Observation of critical phenomena in parity-time-symmetric quantum dynamics, Phys. Rev. Lett. **123**, 230401 (2019).